obtain

$$I(h_3)=\psi^2\cdot\frac{2\varrho-1}{4\varrho}\cdot\frac{1-\varrho^2}{1-2\varrho\cos[\pi h_3(1-\gamma\delta)]+\varrho^2}+\psi^2\cdot\frac{2\varrho+1}{4\varrho}\cdot\frac{1-\varrho^2}{1+2\varrho\cos[\pi h_3(1-\gamma\delta)]+\varrho^2}$$
$$\text{for}\quad H-K\neq 0 \bmod 3\,,\quad \delta\ll 1\,. \quad (41)$$

The first term on the right hand side of equation (41) represents a symmetrically broadened peak at $h_3=L(1-\gamma\delta)^{-1}$ for L even, while the second represents a symmetrically broadened peak at $h_3=(1-\gamma\delta)^{-1}$ for L odd. There is thus a peak shift which in 2θ coordinates is given by

$$\Delta(2\theta)^\circ=+\frac{360}{\pi}\cdot\frac{L^2d^2}{c^2}\cdot(\tan\theta)\cdot\gamma\delta$$
$$\text{for}\quad H-K\neq 0 \bmod 3\,,\quad \delta\ll 1\,. \quad (42)$$

Conclusions

To summarize the results, we find that spacing faults give rise to peak shifts for all reflexions which are equivalent to a change of the c parameter to $c(1+\alpha\delta)$. There are no changes in the integrated intensity and the reflexions remain sharp and symmetrical. The results for layer faults are slightly complicated in that reflexions with $H-K=0$ mod 3 are shifted twice as much as those with $H-K\neq 0$ mod 3 and in the opposite direction. Again, the integrated intensity or the broadening is not affected by layer faults.

An estimate of $\alpha\delta$ can be obtained from measurements of peak shifts for spacing as well as layer faults. In the case of layer faults the parameter α can be estimated independently from measurements of the integral breadths. Inserting this value in $\alpha\delta$, one can obtain δ.

Finally, we note that since deformation stacking faults give rise to changes in integrated intensity and to peak broadening but not to peak shifts, estimates of α are not affected by changes in layer spacing at the faults.

The author is grateful to Dr T. R. Anantharaman, Professor and Head, Department of Metallurgy, Banaras Hindu University, for encouragement and to the University Grants Commission, New Delhi, for the award of a Senior Research Fellowship.

References

CHRISTIAN, J. W. (1954). *Acta Cryst.* **7**, 415.
GEVERS, R. (1954). *Acta Cryst.* **7**, 337.
JAGODZINSKI, H. (1949). *Acta Cryst.* **2**, 201.
LELE, S. (1969). *Acta Cryst.* A**25**, 351.
LELE, S., ANANTHARAMAN, T. R. & JOHNSON, C. A. (1967). *Phys. Stat. Sol.* **20**, 59.
WAGNER, C. N. J., TETELMAN, A. S. & OTTE, H. M. (1962). *J. Appl. Phys.* **33**, 3080.
WARREN, B. E. (1959). *Progr. Met. Phys.* **8**, 147.

Acta Cryst. (1970). A**26**, 349

Contrast Reversal of Kikuchi Lines with Specimen Thickness

BY YASUO NAKAI

Department of Physics, Nagoya University, Nagoya, Japan

(*Received* 29 *May* 1969 *and in revised form* 11 *August* 1969)

In normal Kikuchi patterns a defect line and an excess line pass through the incident spot and a diffracted spot respectively, when the Bragg condition is satisfied. By means of selected area diffraction at 80 kV accelerating voltage, Kikuchi patterns were recorded from various thicknesses of a silicon crystal. Normal contrast was obtained from regions where the thickness was $(n+\frac{1}{2})l$, where l is the extinction distance and n is an integer, while the contrast was reversed for those regions where the thickness was nl. This result, can be explained by a theory of inelastic scattering; it is contrary to that obtained by Thomas & Bell (*Proc. Fourth European Regional Conf. Electron Microscopy*, Rome (1968), 283) where normal contrast was obtained for nl and reversed contrast for $(n+\frac{1}{2})l$.

1. Introduction

Electron diffraction patterns from fairly thick specimens (several thousand Ångstrom) consist of Bragg spots and Kikuchi patterns. Kikuchi (1928) interpreted Kikuchi lines as being the interference pattern from Bragg reflexion of inelastically scattered electrons, and the main features of their geometry and contrast (excess or defect) were explained by this simple theory.

Secondary maxima in the Kikuchi lines similar to those observed in the case of diffraction spots were observed by Uyeda, Fukano & Ichinokawa (1954) in diffraction patterns from a thin film of molybdenite. Kainuma's (1955) theory of Kikuchi lines explains

these secondary maxima qualitatively. Gjønnes & Watanabe (1966) later studied the fine structure of Kikuchi lines in detail and showed that it depends on the deviation from the Bragg condition of the incident beam.

Recently, Thomas & Bell (1968) studied the thickness dependence of the Kikuchi line contrast using the selected area diffraction technique, and concluded that normal Kikuchi line contrast was obtained from regions of the crystal where the thickness was nl, while the contrast was reversed for regions where the thickness was $(n \pm \frac{1}{4})l$, where l is the extinction distance and n an integer. This conclusion is inconsistent with the fact that the contrast of extinction fringes formed by the inelastically scattered electrons is similar to that for the elastically scattered electrons (Kamiya & Uyeda, 1961; Watanabe, 1964). The purpose of the present work is to re-examine the conclusion of Thomas & Bell: the present result, contrary to their conclusion, is that the contrast of a Kikuchi line is reversed as the thickness of the crystal increases by an odd multiple of a half of the extinction distance. This can be explained by the theory of inelastic scattering of Fujimoto & Kainuma (1963).

2. Experiment

Low-angle wedge-shaped silicon specimens prepared by chemical etching (Laurence & Koehler, 1965) were used for the production of Kikuchi patterns for various crystal thicknesses. The selected area diffraction technique at 80 kV was applied throughout the experiment. The size of the selector aperture was about $18 \times 4{\cdot}5\mu$, which corresponded to about $0{\cdot}8 \times 0{\cdot}2\mu$ on the specimen plane.

The following precautions were taken for the correct operation of selected area diffraction. First, the focal length of the objective lens was set so that the first intermediate image produced by the objective lens was formed exactly on the selector aperture, as shown in Fig. 1(*a*). Otherwise, selected areas on the specimen plane would not be the same for different points of the diffraction pattern, as illustrated in Fig. 1(*b*), in which parts A' and B' are the selected areas for the incident ray converging to O' and the diffracted ray converging to H' respectively.

An error similar to that mentioned above may also arise from spherical aberration of the objective lens. Even when the image due to the transmitted beam is focused on the selector aperture, as shown in Fig. 2, the selected area for the ray converging to H' is shifted from that for the axial ray by a distance δ, in the opposite direction to the reciprocal lattice vector corresponding to H'. This results in an effective change of crystal thickness at that region which gives the diffracted ray passing through the selector aperture. The formula for spherical aberration (Hirsch, Howie, Nicholson, Pashley & Whelan, 1965) leads to $\delta = C_s\alpha^3$, where C_s is the spherical aberration constant and α, the scattering angle. In the present experiment C_s is about 5 mm and α is $4{\cdot}8 \times 10^{-2}$ rad for 440 reflexion at an accelerating voltage of 80 kV. Therefore δ is about $0{\cdot}5\mu$, which is not negligible compared with the size of the selected area. In the present experiment, that part of the crystal was used where the extinction fringes were

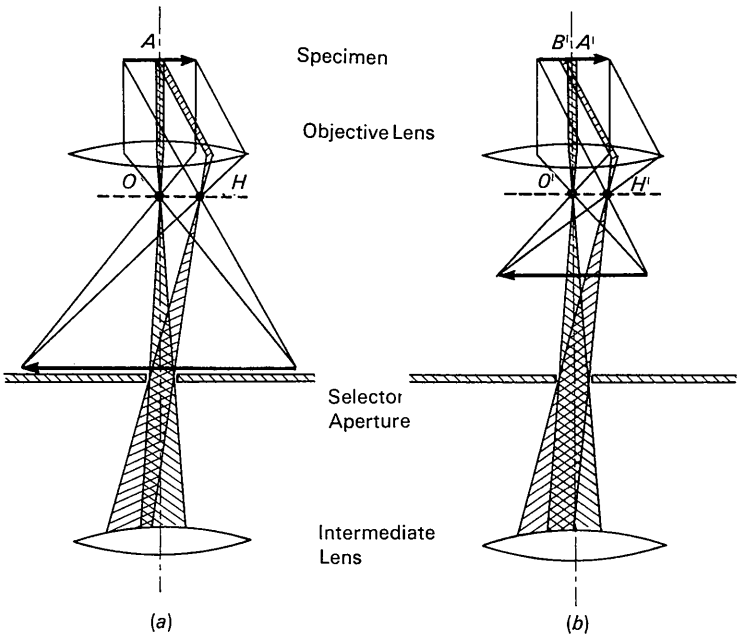

Fig. 1. The first intermediate image produced by the objective lens; (*a*) correct operation of selected area diffraction; (*b*) incorrect operation.

nearly parallel to the reciprocal lattice vector of the relevant reflexion. Thus the shift did not result in a change of thickness in the regions giving rise to the incident and diffracted rays.

The leakage magnetic field of the intermediate lens may deflect the first intermediate image produced by the objective lens. When the lens current of the intermediate lens is changed from the value for microscopy to that for diffraction, the first intermediate image is usually shifted. The shift measured in the present instrument was less than $0{\cdot}2\mu$ perpendicular to the extinction fringes. The effect of the deflecting field was neglected.

3. Results

Fig. 3 and 4 are bright-field images and corresponding diffraction patterns at the Bragg reflecting positions 220 and 111 respectively. The small rectangular area on each micrograph indicates the position and size of the selector aperture. The experimental results are summarized as follows.

(i) When the selector aperture is placed on a dark fringe, where the thickness is $(n+\frac{1}{2})l$ [Fig. 3(*a*)], normal Kikuchi patterns are obtained, *i.e.* defect and excess Kikuchi lines go through the incident and diffracted spots respectively.

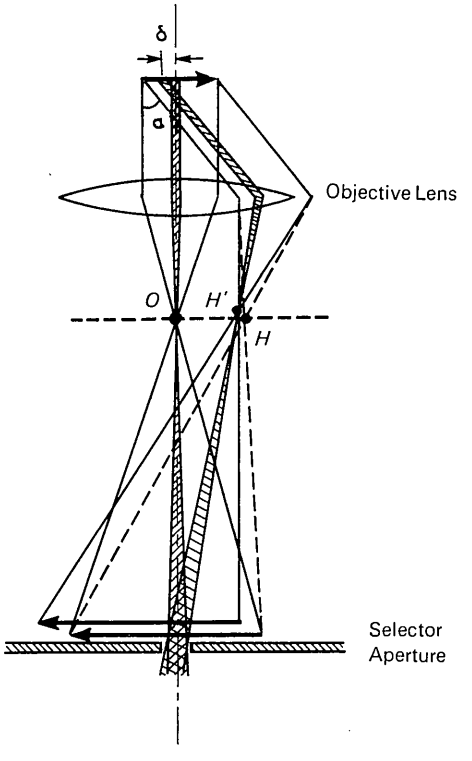

Fig. 2. The shift of the selected area caused by spherical aberration. δ: the shift of the selected area; α: the scattering angle; O, H: foci of the rays in the ideal lens; H': real focus of the non-axial ray.

(ii) When the selector aperture is placed on a bright fringe, where the thickness is nl [Fig. 3(*c*)], the contrast of the Kikuchi pattern is reversed.

(iii) When the selector aperture is placed between bright and dark fringes, there are two cases: a crystal thickness of $(n+\frac{1}{4})l$ [Fig. 3(*d*)] and a crystal thickness of $(n-\frac{1}{4})l$ [Fig. 3(*b*)]. In the former case the Kikuchi pattern looks similar to that of case (ii) and in the latter, similar to that of case (i).

Fig. 5 shows the diffraction pattern when the first intermediate image is formed not exactly on the selector aperture. Two kinds of contrast effect are observed, as illustrated in Fig. 6(*a*), *i.e.* one is similar to the extinction contour from a bent crystal [parts *A* and *B* in Fig. 6(*a*)] and the other is similar to that from a perfect crystal [part *C* in Fig. 6(*a*)]. It should be noted that the contrast is reversed in the left and right halves of the photograph, along the line parallel to *pp'* [Fig. 6(*a*)] which corresponds to the locus of equal thickness.

As described in § 2, the area selected by the aperture depends on the position of the diffraction pattern in this case. The diffraction pattern near points *O*, *A*, *B* and *H* of Fig. 6(*a*) is considered to be produced from parts *O'*, *A'*, *B'* and *H'* of the specimen as shown in Fig. 6(*b*).

4. Discussion

(i) *Comparison with the experiments of Thomas & Bell*

Although Thomas & Bell first pointed out the contrast reversal of Kikuchi lines, their results and ours are quite different in the local variation of detailed contrast. They reported that the Kikuchi line from a bright fringe gives normal contrast (defect line through the transmitted spot and excess line through the diffracted spot), whereas the result of the present experiment shows that the Kikuchi line from a dark fringe gives normal contrast. According to Thomas & Bell the contrast of a Kikuchi line is reversed from normal when the selector aperture is moved from a bright fringe to a position corresponding roughly to a crystal thickness equal to an odd multiple of a quarter the extinction distance. In the present experiment, on the other hand, the contrast reversal is observed when the selector aperture is moved from a dark fringe to a bright fringe. The variation of contrast is more marked for the 220 reflexion (Fig. 3) than for the 111 reflexion (Fig. 4). In the case of the 111 reflexion, the secondary maxima on the Kikuchi line is quite noticeable because of the large structure factor and the small Bragg angle. This gives rise to the complicated Kikuchi lines for the deviated Bragg reflexion position. Care is necessary not to confuse the secondary maxima with the principal maximum.

(ii) *Comparison with theory*

Fujimoto & Kainuma (1963) and Fukuhara (1963) discussed the intensity of diffraction patterns from inelastic scattering for the case where the incident beam satisfies a Bragg condition. Although these theories

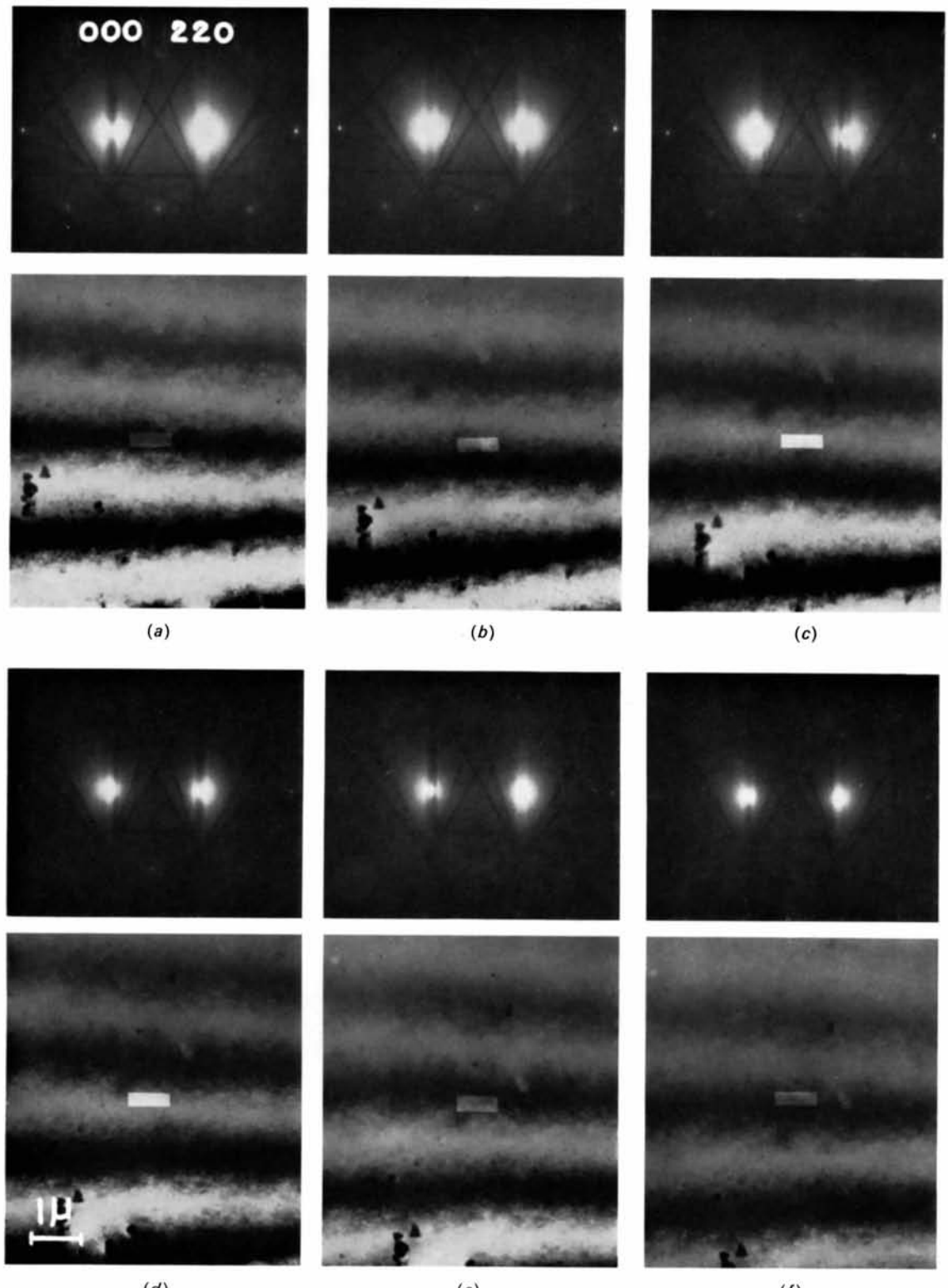

Fig. 3. Bright-field images and corresponding diffraction patterns of silicon taken under 220 reflexion conditions at 80 kV. A small rectangular area on each micrograph indicates the selector aperture.

[*To face p.* 351

used different methods of solving the equation for inelastic waves, Kainuma (1965) showed that the two methods are equivalent. This means that these theories would give the same result if the same assumption were used for the energy-momentum relation.

In both theories, energy conservation between the elastic wave, the inelastic wave and the wave excited in the crystal, is assumed to hold, while momentum conservation between the three waves does not always hold because of the finite crystal thickness. However, the inelastic waves which satisfy the momentum conservation condition make the main contribution to the final intensity.

In Fujimoto & Kainuma's theory, waves with various wave-vectors are excited in the crystal to give inelastic scattering with a definite energy loss, while in Fukuhara's theory, a definite relation is assumed between the energy and the wave vector of the wave excited in the crystal. These different energy–momentum relations result in different intensity distributions in the diffraction pattern.

By use of equation (37) of Fujimoto & Kainuma's theory and equation (20) of Fukuhara's theory the intensity curves near the transmitted and diffracted spots were calculated for a crystal thickness of four times the extinction distance. The results are shown in Fig. 7. Fujimoto & Kainuma's theory gives stronger background intensity than Fukuhara's theory because the energy–momentum relationship in the latter theory provides very little momentum conservation for large angle scattering, and therefore gives very weak background. The above two theories give different widths for a Kikuchi line: the former theory gives the same width for a Kikuchi line near the incident spot and that near a diffracted spot, while the latter theory gives different widths. The result of the latter theory is found to be very different from the experimental result. This implies that the assumption of a definite energy–momentum relationship is inadequate for an interpretation of the present result. Therefore, in the following, the theory of Fujimoto & Kainuma was used for comparison with the experimental results.

Equation (37) of Fujimoto & Kainuma's theory is given as

$$I_g' = C_1 + C_2\frac{\sin(dD)}{(dD)} + C_3\frac{\sin(d'D)}{(d'D)} + C_4\frac{\sin\left(\frac{d'-d}{2}D\right)}{\left(\frac{d'-d}{2}D\right)}\cos\left(\frac{d'+d}{2}D\right) + C_5\frac{\sin(d'D)+\sin(dD)}{(d'+d)D},$$

where C_{1-5} are monotonic functions of the parameters W and W' which indicate the deviation from the Bragg condition for elastic and inelastic waves, D is the thickness of the crystal and d and d' are defined as

$$d = 2\pi l\sqrt{1+\bar{W}^2}$$
$$d' = 2\pi l\sqrt{1+\bar{W}'^2}$$

where l is the extinction distance.

For small angle inelastic scattering, such as that due to plasmon excitation, the main terms are the first and fourth, and the other terms are negligible. The first term gives the background and the fourth term the main part of the intensity of the Kikuchi line. The contrast similar to the bent extinction contour in Fig. 5 is explained by the fourth term. This term becomes $C_4\cos(dD)$ for small values of $|W'-W|$, and gives the contrast reversal with a change in thickness of half the extinction distance.

For large angle inelastic scattering the main terms are the first and second, because in the large angle

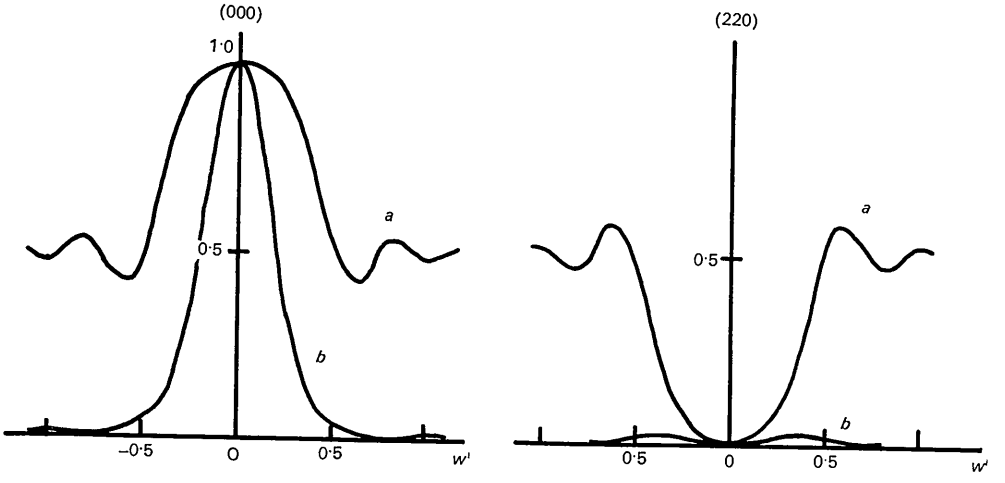

Fig. 7. Calculated intensity profiles of the Kikuchi line near the transmitted and diffracted spots for the 220 reflexion. *a:* Fujimoto & Kainuma's theory, $A_{NN',l}(q) = C$ (C: constant), $W=0$, $D=4d$. *b:* Fukuhara's theory, U_q=const., $W=0$, $t=4V_h/k_0$. The notation is the same as that in the original papers.

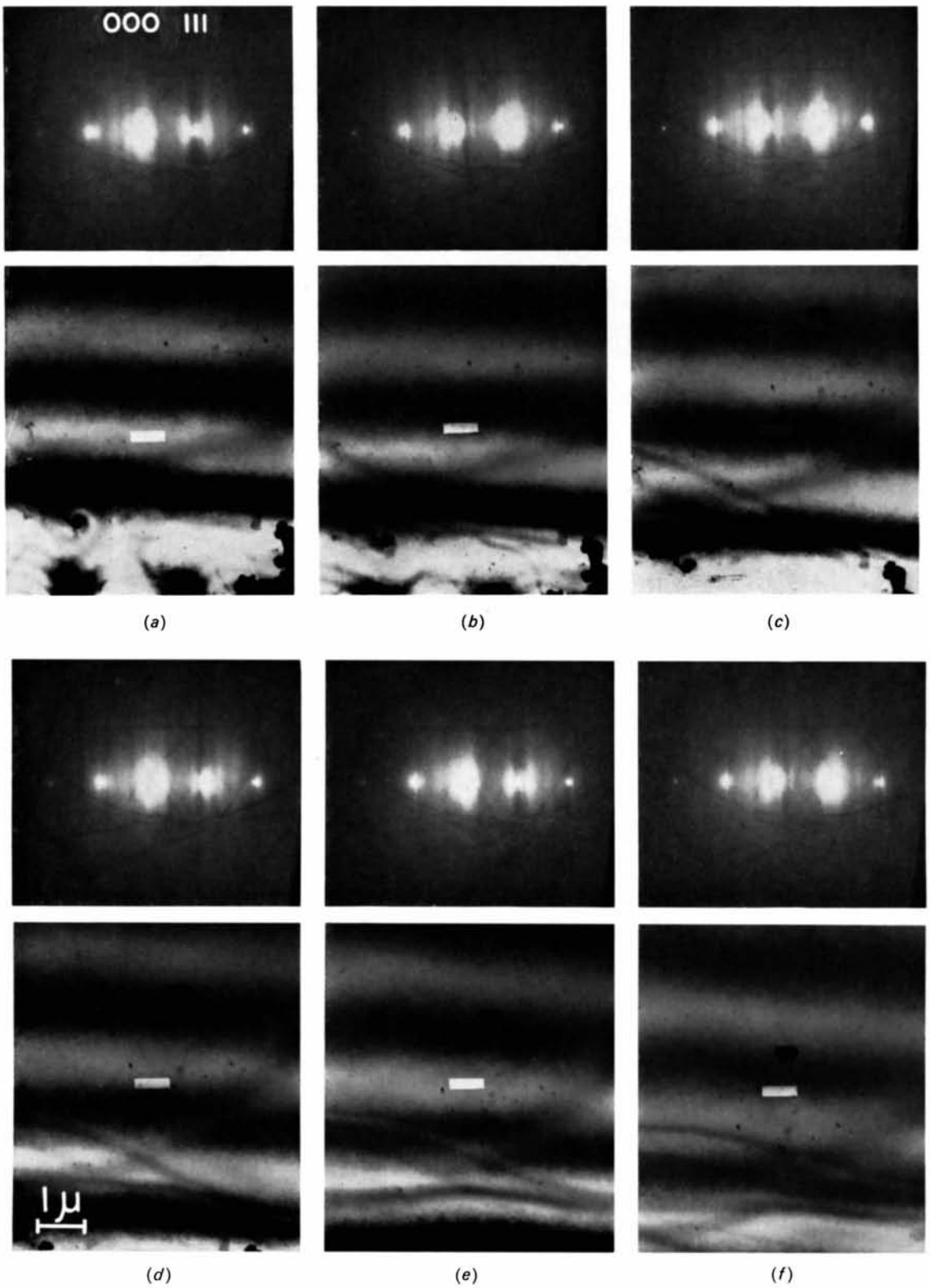

Fig. 4. Bright-field images and corresponding diffraction patterns of silicon taken under 111 reflexion conditions at 80 kV.

[To face p. 352

Fig. 5. Diffraction pattern of silicon obtained under conditions such those shown in Fig. 1(*b*), at 80 kV. The Bragg condition is not exactly satisfied for the 111 reflexion. Two kinds of contrast effect are observed, as illustrated in Fig. 6(*a*).

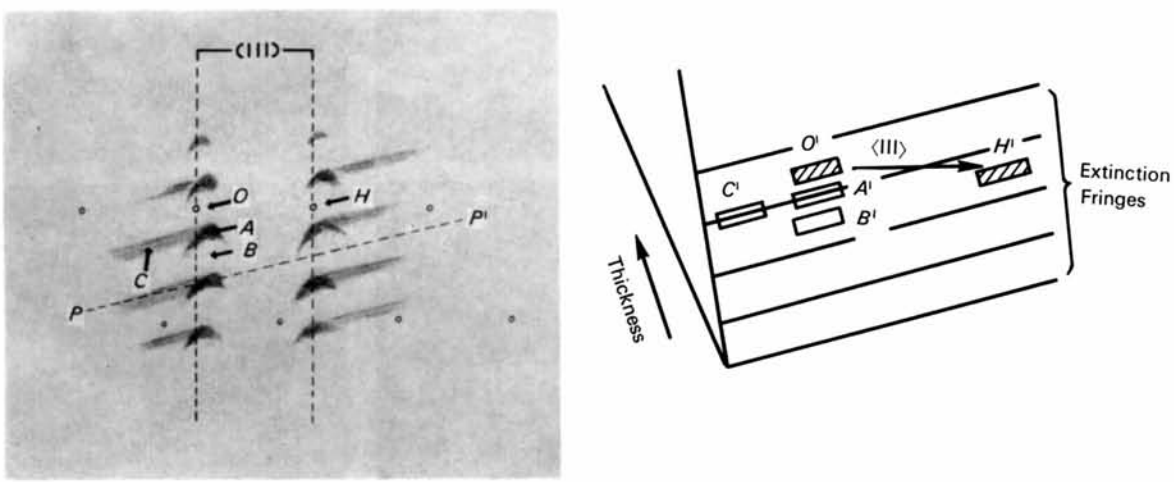

(*a*) (*b*)

Fig. 6. (*a*) Contrast for the conditions of Fig. 5. (*b*) Illustration of the selected area corresponding to Fig. 5.

scattering region the value of d' is much larger than that of d, and C_1 and C_2 are larger than C_3, C_4 and C_5. The second term gives the contrast corresponding to that apparent in part C of Fig. 6(a).

In Fujimoto & Kainuma's theory the fourth term in their equation (37) is due to the intra-branch scattering. As is well known (Howie, 1962; Fujimoto& Howie, 1966), this shows that the intra-branch scattering contributes mainly to the contrast effect in the small scattering-angle region. The second term corresponds to the interaction between intra-branch and inter-branch scattering. A detailed examination of this term shows that the inter-branch inelastic scattering contributes considerably to the contrast effect in the large-angle scattering region as shown in Figs. 5 and 6(a).

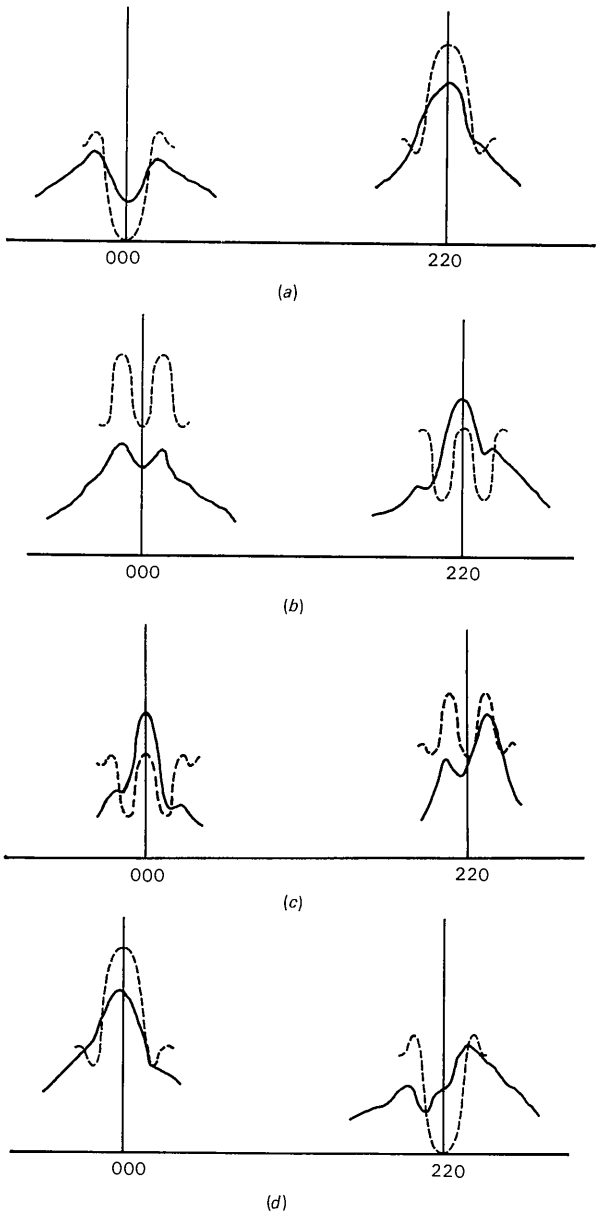

Fig. 8. Densitometer curves corresponding to Fig. 3 and theoretical curves (broken lines). (a), (b), (c) and (d) correspond to Fig. 3(a), (b), (c) and (d) respectively.

The densitometer curves of Fig. 3(a), (b), (c) and (d) are reproduced in Fig. 8(a), (b), (c) and (d) respectively. The broken curves in Fig. 8 are the result of numerical calculations using Fujimoto & Kainuma's theory for the case where the Bragg condition for the 220 reflexion is exactly satisfied. The extinction distance is assumed to be 650 Å. The intensity is normalized so that the theoretical background coincides with the average of the intensity maximum and minimum of the 000 and 220 Kikuchi lines. The contrast reversal of theKikuchi lines observed in this experiment is successfully explained by the theory, as seen in Fig. 8.

Some deviations are shown in the detailed profiles of Fig. 8. The reasons for this may be as follows: (1) In the calculation the scattering cross-section is assumed to be independent of the scattering angle, and *Umklapprozess* is neglected for simplicity; (2) the Bragg condition is not exactly satisfied experimentally because of technical difficulties; (3) multiple inelastic scattering contributes to the diffraction patterns; (4) the thickness is not exactly uniform in the selected area. The absorption effect and many-beam effect must be also taken into account for detailed comparison.

The author would like to express his sincere thanks to Professor R. Uyeda and Dr Y. Kamiya for encouragement and kind guidance. He also expresses his thanks to Professor Y. Kainuma for helpful discussions.

References

FUJIMOTO, F. & KAINUMA, Y. (1963). *J. Phys. Soc. Japan*, **18**, 1792.
FUJIMOTO, F. & HOWIE, A. (1966). *Phil. Mag.* **2**, 1131.
FUKUHARA, A. (1963). *J. Phys. Soc. Japan*, **18**, 496.
GJØNNES, J. & WATANABE, D. (1966). *Acta Cryst.* **21**, 297.
HIRSH, P. B., HOWIE, A., NICHOLSON, R. B., PASHLEY, D. W. & WHELAN, M. J. (1965). *Electron Microscopy of Thin Crystals*. London: Butterworths.
HOWIE, A. (1962). *Proc. Roy. Soc.* A **271**, 268.
KAINUMA, Y. (1965). *J. Phys. Soc. Japan*, **20**, 2263.
KAMIYA, Y. & UYEDA, R. (1961). *J. Phys. Soc. Japan*, **16**, 1361.
KIKUCHI, S. (1928). *Japan. J. Phys.* **5**, 83.
LAURENCE, J. E. & KOEHLER, H. (1965). *J. Sci. Instrum.* **42**, 270.
THOMAS, G. & BELL, W. L. (1968). *Proc. Fourth European Regional Conf. on Electron Microscopy, Rome*. p. 283.
UYEDA, R., FUKANO, Y. & ICHINOKAWA, T. (1954). *Acta Cryst.* **7**, 217.
WATANABE, H. (1964). *Japan. J. Appl. Phys.* **3**, 480.